

Article

Weakly Bound Dimer of a Diaryloxygermylene Derived from a ^tBuPh₂Si-Substituted 2,2'-Methylenediphenol

Ryo Yamazaki ¹, Ryunosuke Kuriki ¹, Asuka Sugihara ¹, Youichi Ishii ¹  and Takuya Kuwabara ^{1,2,*} 

¹ Department of Applied Chemistry, Faculty of Science and Engineering, Chuo University, 1-13-27, Kasuga, Bunkyo-ku, Tokyo 112-8551, Japan; a16.s6kp@g.chuo-u.ac.jp (R.Y.); a14.hr7c@g.chuo-u.ac.jp (R.K.); a17.rtwm@g.chuo-u.ac.jp (A.S.); yo-ishii@kc.chuo-u.ac.jp (Y.I.)

² Department of Chemistry and Biochemistry, Faculty of Humanities and Sciences, Ochanomizu University, 2-1-1, Otsuka, Bunkyo-ku, Tokyo 112-8610, Japan

* Correspondence: kuwabara.takuya@ocha.ac.jp

Abstract: Novel diaryloxygermylenes have been prepared by the reaction of Lappert's germylene, Ge[N(SiMe₃)₂]₂, with 2,2'-methylenediphenols bearing different substituents. The bulkiness of the substituents on the ortho positions of the phenolic oxygen (6 and 6' positions) affects the structure of the products both in the solid-state and in solution. When the ortho substituents are Si^tBuPh₂, the diaryloxygermylene crystalizes as a weakly bound dimer with intermolecular Ge...O distances of ca. 3.0 Å and exists as a monomer in solution. In contrast, the germylene with SiMePh₂ groups as the ortho substituents form a tightly bound dimer featuring a Ge₂O₂ rhombus with cis-oriented terminal aryloxy groups in the crystalline state, which is confirmed to be maintained in solution through the VT (variable-temperature)-¹H NMR studies. To the best of our knowledge, the former dimeric structure is unprecedented in the family of dioxytetrylenes.

Keywords: germylene; crystal structure; aryloxy ligand; dimeric structure



Citation: Yamazaki, R.; Kuriki, R.; Sugihara, A.; Ishii, Y.; Kuwabara, T. Weakly Bound Dimer of a Diaryloxygermylene Derived from a ^tBuPh₂Si-Substituted 2,2'-Methylenediphenol. *Crystals* **2022**, *12*, 605. <https://doi.org/10.3390/cryst12050605>

Academic Editor: Paola Paoli

Received: 23 March 2022

Accepted: 22 April 2022

Published: 25 April 2022

Publisher's Note: MDPI stays neutral with regard to jurisdictional claims in published maps and institutional affiliations.



Copyright: © 2022 by the authors. Licensee MDPI, Basel, Switzerland. This article is an open access article distributed under the terms and conditions of the Creative Commons Attribution (CC BY) license (<https://creativecommons.org/licenses/by/4.0/>).

1. Introduction

Divalent heavier group 14 element species (:ER₂, E = Si, Ge, Sn, Pb), so-called tetrylenes or metallylenes, have gained increasing attention due to their potential for mimicking the reactivities of transition metals [1–4]. Since tetrylenes are highly reactive, judicious choice of the substituents is essential to isolate such species. After the seminal work of Lappert utilizing bulky -N(SiMe₃)₂ and -C(SiMe₃)₃ groups as the substituents for Ge(II), Sn(II) and Pb(II) species [5,6], various types of substituents that enable isolation of tetrylenes have been explored, for instance, *m*-terphenyl [7,8], Rind (1,1,3,3,5,5,7,7-octa-R-substituted *s*-hydrindacenyl) [9], Trp* (extended 9-triptycyl) [10], and boryl groups [11,12], just to name a few. In contrast with these B-, C- and N-based substituents that can bring two or three pendant substituents, O-based substituents offer only one pendant substituent. Thus, most of O-disubstituted tetrylenes (dioxytetrylenes; :E(OR)₂) easily form a dimer [13], trimer [14–16], tetramer [16] or polymer [14,17], due to the lack of steric protection. However, isolation of two-coordinate dioxytetrylenes has been achieved by utilizing bulky OR groups, where R = *m*-terphenyl [13,18–21], 2,6-dialkylphenyl [22,23], binaphthyl [24], boryl [25,26] substituents, and so on.

Recently, our group has demonstrated that a tetrathiacalix[4]arene-supported stannylenes and plumblylenes have a two-coordinate metal center with an E(OAr)₂ substructure (E = Sn, Pb) [27], which is in stark contrast to the tetra-coordinated Ge(II) and Sn(II) centers found in the related 1,3-diether of calix[4]arene-tetrylenes reported by Parkin and his co-workers [28,29]. It has also been reported that germylenes and stannylenes incorporated in calix[*n*]arene scaffolds, where *n* = 4, 5, 8, feature a Ge₂O₂ and Sn₂O₂ rhombi in the solid-state [30–32]. Based on these studies on calixarene-tetrylene compounds, we next became interested in the structure of diaryloxytetrylenes derived from

2,2'-methylenediphenol derivatives that can be viewed as a partial structure of calixarenes. Although transition metal complexes bearing fragment structure of calixarenes have been well-investigated [33–38], their tetrylene counterparts have not been reported so far. In this contribution, we report the synthesis and solid-state structures of two novel diaryloxygermylenes derived from 2,2'-methylenediphenols with bulky silyl substituents on the ortho positions of the phenolic oxygen atoms. One of the products has a weakly bound dimeric structure in the solid state, which is, as far as we know, unprecedented in the solid-state structure of related dioxytetrylenes. The other one crystallizes as an O-bridged dimer where the terminal OAr groups are oriented in a cis-fashion. Solution behavior of the products has also been investigated by VT-¹H NMR studies.

2. Materials and Methods

2.1. General Procedures

All manipulations were performed under an argon atmosphere by using standard Schlenk techniques or a conventional glovebox. Toluene, hexane, and toluene-*d*₈ were dried with a potassium mirror before use. Dichloromethane (CH₂Cl₂) and chloroform-*d*₁ were dried over P₄O₁₀, distilled, degassed, and stored under argon with molecular sieves. Unless otherwise specified, commercially available compounds were used as received. Ge[N(SiMe₃)₂]₂ was synthesized by the literature method [6]. ¹H (500 MHz), ¹³C{¹H} (126 MHz), and ²⁹Si{¹H} (98 MHz) NMR spectra were recorded on a JEOL ECZ-500 spectrometer at 20 °C unless otherwise stated. Chemical shifts are reported in δ and referenced to residual ¹H and ¹³C signals of the deuterated solvents as internal standards or to the ²⁹Si NMR signal of SiMe₄ in CDCl₃ (δ 0). Elemental analyses were performed on a Perkin Elmer 2400 series II CHN analyzer.

2.2. Synthesis of 2-(*tert*-Butyldiphenylsilyl)-4-methylphenol (**1a**)

Imidazole (1.3607 g, 19.98 mmol) and ^tBuPh₂SiCl (1.38 mL, 5.00 mmol) were added to a CH₂Cl₂ solution (15 mL) of 2-bromo-4-methylphenol (0.62 mL, 5.14 mmol). After stirring at r.t. for 24 h, the resulting mixture was poured into a saturated aqueous solution of NH₄Cl and extracted with CH₂Cl₂. The organic layer was dried over MgSO₄ and concentrated under reduced pressure. Rough purification by silica gel column chromatography (eluent = hexane) followed by removal of the solvent provided a colorless oil (1.9 g) that was used directly for retro-Brook rearrangement. The oil (1.9 g) was dissolved in THF (7 mL), and the solution was cooled to −78 °C. ⁿBuLi (1.57 M in hexane; 3.2 mL, 4.9 mmol) was added dropwise to the solution, and the mixture was stirred for 30 min at this temperature and then 24 h at room temperature. After removal of the volatiles under reduced pressure, the residue was extracted by CH₂Cl₂/NH₄Cl(aq). The organic layer was dried over MgSO₄, and the solvent was removed in vacuo. The crude mixture was washed with hexane to give analytically pure **1a** as a white powder (1.700 g, 4.90 mmol, 95% over two steps). ¹H NMR (CDCl₃): δ 7.65 (dd, ³J = 8.5 Hz, ⁴J = 1.5 Hz, 4H, Si–Ph(*o*)), 7.44 (tt, ³J = 7.5 Hz, ⁴J = 1.5 Hz, 2H, Si–Ph(*p*)), 7.39 (t, ³J = 7.5 Hz, 4H, Si–Ph(*m*)), 7.30 (d, ⁴J = 2.0 Hz, 1H, C(3)–H), 7.16 (dd, ³J = 8.0 Hz, ⁴J = 2.0 Hz, 1H, C(5)–H), 6.72 (d, ³J = 8.0 Hz, 1H, C(6)–H), 4.77 (s, 1H, OH), 2.27 (s, 3H, ArMe), 1.23 (s, 9H, ^tBu); ¹³C{¹H} NMR (CDCl₃): δ 159.1 (s, 4°, C(1)–OH), 138.1 (s, 3°, C(3)), 136.4 (s, 3°, C(*o*) of SiPh), 134.5 (s, 4°, C(*ipso*) of SiPh), 132.5 (s, 3°, C(5)), 129.8 (s, 3°, C(*p*) of SiPh), 129.3 (s, 4°, C(4)), 128.3 (s, 3°, C(*m*) of SiPh), 118.9 (s, 4°, C(2)), 116.1 (s, 3°, C(6)), 29.2 (s, 1°, ^tBu), 20.9 (s, 1°, ArMe), 18.9 (s, 4°, ^tBu); ²⁹Si NMR (CDCl₃): δ −7.2 (s). Anal. Calcd for C₂₃H₂₆O_{Si} (**1a**): C, 78.72, H, 7.56. Found: C, 79.13, H, 7.86.

2.3. Synthesis of 2-(Methyldiphenylsilyl)-4-methylphenol (**1b**)

Imidazole (1.3615 g, 19.99 mmol) and MePh₂SiCl (1.05 mL, 5.00 mmol) were added to a CH₂Cl₂ solution (15 mL) of 2-bromo-4-methylphenol (0.60 mL, 4.97 mmol). After heating at 40 °C for 24 h, the resulting mixture was poured into a saturated aqueous solution of NH₄Cl and extracted with CH₂Cl₂. The organic layer was dried over MgSO₄, and the solvent was removed in vacuo. Rough purification by silica gel column chromatography

(eluent = hexane:EtOAc = 15:1) provided a colorless oil (687.1 mg) that was directly used for retro-Brook rearrangement. The oil was dissolved in THF (7 mL), and the solution was cooled to $-78\text{ }^{\circ}\text{C}$. $n\text{-BuLi}$ (1.57 M in hexane; 1.37 mL, 2.15 mmol) was added dropwise to the solution, and the mixture was stirred for 30 min at this temperature and then 24 h at room temperature. After removal of the volatiles under reduced pressure, the residue was extracted by $\text{CH}_2\text{Cl}_2/\text{NH}_4\text{Cl}(\text{aq})$. The organic layer was dried over MgSO_4 , and the solvent was removed in vacuo. The crude mixture was washed with hexane to give analytically pure **1b** as a white powder (303.7 mg, 0.998 mmol, 20% over two steps). $^1\text{H NMR}$ (CDCl_3): δ 7.58 (d, $^3J = 7.5\text{ Hz}$, 4H, Si-Ph(*o*)), 7.45–7.37 (m, 6H, Si-Ph(*p, m*)), 7.13 (dd, $^3J = 8.5\text{ Hz}$, $^4J = 2.5\text{ Hz}$, 1H, C(5)-H), 7.06 (d, $^4J = 2.5\text{ Hz}$, 1H, C(3)-H), 6.68 (d, $^3J = 8.5\text{ Hz}$, 1H, C(6)-H), 4.88 (s, 1H, OH), 2.24 (s, 3H, ArMe), 0.88 (s, 3H, SiMe); $^{13}\text{C}\{^1\text{H}\}$ NMR (CDCl_3): δ 158.8 (s, 4° , C(1)-OH), 137.3 (s, 3° , C(3)), 135.9 (s, 4° , C(*ipso*) of SiPh), 135.3 (s, 3° , C(*o*) of SiPh), 132.6 (s, 3° , C(5)), 129.83 (s, 3° , C(*p*) of SiPh), 129.78 (s, 4° , C(4)), 128.3 (s, 3° , C(*m*) of SiPh), 120.7 (s, 4° , C(2)), 115.6 (s, 3° , C(6)), 20.7 (s, 1° , ArMe), -2.94 (s, 1° , SiMe), $^{29}\text{Si NMR}$ (CDCl_3): δ -13.1 (s). Anal. Calcd for $\text{C}_{20}\text{H}_{20}\text{OSi}$ (**1b**): C, 78.90, H, 6.62. Found: C, 78.81, H, 6.61.

2.4. Synthesis of 2,2'-Methylenebis[6-(*tert*-butyldiphenylsilyl)-4-methylphenol] (**2a**)

A solution of **1a** (1.2003 g, 3.464 mmol) in Et_2O (18 mL) was cooled to $0\text{ }^{\circ}\text{C}$. To this solution, MeMgBr (1.0 M in THF; 3.09 mL, 3.09 mmol) was added dropwise, and the mixture was warmed up to r.t. and stirred for 30 min. Volatiles were removed under reduced pressure, and then toluene (20 mL) and paraformaldehyde (46.7 mg, 1.55 mmol) were added. This solution was stirred for 14 h at $80\text{ }^{\circ}\text{C}$, and the resultant mixture was extracted with Et_2O . The organic layer was washed with $\text{NH}_4\text{Cl}(\text{aq})$, dried over MgSO_4 , and evaporated to give a crude product, which was further purified by silica gel column chromatography (eluent = hexane: $\text{CH}_2\text{Cl}_2 = 3:1$) to afford **2a** as a white powder (842.4 mg, 1.19 mmol, 69%). $^1\text{H NMR}$ (CDCl_3): δ 7.53 (dd, $^3J = 8.5$, $^4J = 1.4\text{ Hz}$, 8H, Si-Ph(*o*)), 7.37 (tt, $^3J = 7.5$, $^4J = 1.4\text{ Hz}$, 4H, Si-Ph(*p*)), 7.29 (t, $^3J = 7.5\text{ Hz}$, 8H, Si-Ph(*m*)), 7.16 (d, $^4J = 2.2\text{ Hz}$, 2H, C(3)-H), 7.02 (d, $^4J = 2.2\text{ Hz}$, 2H, C(5)-H), 6.14 (s, 2H, OH), 3.77 (s, 2H, CH_2), 2.21 (s, 6H, ArMe), 1.15 (s, 18H, $t\text{Bu}$); $^{13}\text{C}\{^1\text{H}\}$ NMR (CDCl_3): δ 156.1 (s, 4° , C(1)-OH), 137.0 (s, 3° , C(5)), 136.4 (s, 3° , C(*o*) of SiPh), 134.8 (s, 4° , C(*ipso*) of SiPh), 133.6 (s, 3° , C(3)), 129.68 (s, 4° , C(4)), 129.63 (s, 3° , C(*p*) of SiPh), 128.2 (s, 3° , C(*m*) of SiPh), 126.8 (s, 4° , C(2)), 119.9 (s, 4° , C(6)), 31.5 (s, 2° , CH_2), 29.5 (s, 1° , $t\text{Bu}$), 20.9 (s, 1° , ArMe), 18.9 (s, 4° , $t\text{Bu}$); $^{29}\text{Si NMR}$ (CDCl_3): δ -7.2 (s). Anal. Calcd for $\text{C}_{47}\text{H}_{52}\text{O}_2\text{Si}_2$ (**2a**): C, 80.06, H, 7.43. Found: C, 79.96, H, 7.58.

2.5. Synthesis of 2,2'-Methylenebis[6-(methyl)diphenylsilyl]-4-methylphenol] (**2b**)

A solution of **1b** (502.7 g, 1.651 mmol) in Et_2O (9 mL) was cooled to $0\text{ }^{\circ}\text{C}$. To this solution, MeMgBr (1.0 M in THF; 1.65 mL, 1.65 mmol) was added dropwise, and the mixture was warmed up to r.t. and stirred for 30 min. Volatiles were removed under reduced pressure, and then toluene (10 mL) and paraformaldehyde (25.1 mg, 0.825 mmol) were added. This solution was stirred for 24 h at $80\text{ }^{\circ}\text{C}$, and the resultant mixture was extracted with Et_2O . The organic layer was washed with $\text{NH}_4\text{Cl}(\text{aq})$, dried over MgSO_4 , and evaporated to give a crude product, which was further purified by silica gel column chromatography (eluent = hexane: $\text{CH}_2\text{Cl}_2 = 1:1$) to afford **2b** as a white powder (203.8 mg, 0.328 mmol, 40%). $^1\text{H NMR}$ (CDCl_3): δ 7.50 (dd, $^3J = 8.0$, $^4J = 1.5\text{ Hz}$, 8H, Si-Ph(*o*)), 7.40 (tt, $^3J = 7.5$, $^4J = 1.4\text{ Hz}$, 4H, Si-Ph(*p*)), 7.33 (t, $^3J = 8.0\text{ Hz}$, 8H, Si-Ph(*m*)), 7.15 (d, $^4J = 2.0\text{ Hz}$, 2H, C(3)-H), 6.87 (d, $^4J = 2.0\text{ Hz}$, 2H, C(5)-H), 6.08 (s, 2H, OH), 3.77 (s, 2H, CH_2), 2.20 (s, 6H, ArMe), 0.82 (s, 6H, SiMe); $^{13}\text{C}\{^1\text{H}\}$ NMR (CDCl_3): δ 156.0 (s, 4° , C(1)-OH), 136.0 (s, 3° , C(5)), 135.9 (s, 4° , C(*ipso*) of SiPh), 135.3 (s, 3° , C(*o*) of SiPh), 133.8 (s, 3° , C(3)), 130.3 (s, 4° , C(4)), 129.8 (s, 3° , C(*p*) of SiPh), 128.3 (s, 3° , C(*m*) of SiPh), 126.7 (s, 4° , C(2)), 121.4 (s, 4° , C(6)), 31.3 (s, 2° , CH_2), 20.7 (s, 1° , ArMe), -2.9 (s, 1° , SiMe); $^{29}\text{Si NMR}$ (CDCl_3): δ -11.8 (s). Anal. Calcd for $\text{C}_{41}\text{H}_{40}\text{O}_2\text{Si}_2$ (**2b**): C, 79.31, H, 6.49. Found: C, 78.92, H, 6.59.

2.6. Synthesis of Diaryloxygermylene (3a)

In a J. Young tube, compound **2a** (49.8 mg, 0.071 mmol) was dissolved in hexane (2 mL). Then a solution of $\text{Ge}[\text{N}(\text{SiMe}_3)_2]_2$ (34.1 mg, 0.087 mmol) in hexane (2 mL) was added, and the mixture was heated at 50 °C for 48 h, during which period a white crystalline powder precipitated out. The solvent was removed by a syringe, and the remaining powder was dried under reduced pressure to give **3a** as a white crystalline powder (28.4 mg, 0.037 mmol, 52%). The sample of **3a** thus obtained was spectroscopically pure, although elemental analysis could not be performed because of its high sensitivity toward oxygen and moisture. ^1H NMR (r.t., toluene- d_8): δ 7.61–7.53 (m, 10 H, Si–Ph(*o*) + C(5)–H), 7.10 (d, $^4J = 2.0$ Hz, 2H, C(3)–H), 7.05 (t, $^3J = 7.5$ Hz, 4H, Si–Ph(*p*)), 6.92 (t, $^3J = 7.5$ Hz, 8H, Si–Ph(*m*)), 3.36 (brs, 2H, CH_2), 2.18 (s, 6H, ArMe), 1.24 (s, 18H, ^tBu); ^1H NMR (–60 °C, toluene- d_8): δ 7.68 (s, 2H, C(5)–H), 7.63 (d, $^3J = 7.5$ Hz, 4H, Si–Ph(*o*)), 7.53 (d, $^3J = 7.6$ Hz, 4H, Si–Ph(*o*)), 7.14 (s, 2H, C(3)–H), 7.07–7.03 (m, 4H, Si–Ph(*p*)), 6.90 (t, $^3J = 7.5$ Hz, 4H, Si–Ph(*m*)), 6.84 (t, $^3J = 7.6$ Hz, 4H, Si–Ph(*m*)), 3.46 (d, $^2J = 14.2$ Hz, 1H, CH_2), 3.20 (d, $^2J = 14.2$ Hz, 1H, CH_2), 2.20 (s, 6H, ArMe), 1.29 (s, 18H, ^tBu); $^{13}\text{C}\{^1\text{H}\}$ NMR (r.t., toluene- d_8): δ 161.0 (s, 4°, C(1)–OH), 137.2 (brs, s, 4°, C(*ipso*) of SiPh), 136.4 (s, 3°, C(5)), 136.0 (brs, 3°, C(*o*) of SiPh), 133.3 (s, 3°, C(3)), 129.65 (s, 4°, C(2) or C(4)), 129.60 (s, 4°, C(2) or C(4)), 129.2 (brs, 3°, C(*p*) of SiPh), 128.4 (s, 3°, C(*m*) of SiPh), 122.5 (s, 4°, C(6)), 35.9 (s, 2°, CH_2), 29.2 (s, 1°, ^tBu), 20.9 (s, 1°, ArMe), 19.1 (s, 4°, ^tBu) ^{29}Si NMR (toluene- d_8): δ –7.1 (s).

2.7. Synthesis of Diaryloxygermylene Dimer (3b)

In a J. Young tube, compound **2b** (50.5 mg, 0.081 mmol) was dissolved in hexane (2 mL). Then a solution of $\text{Ge}[\text{N}(\text{SiMe}_3)_2]_2$ (39.3 mg, 0.100 mmol) in hexane (2 mL) was added, and the mixture was heated at 50 °C for 24 h, during which period a white crystalline powder precipitated out. The solvent was removed by a syringe, and the remaining powder was dried under reduced pressure to give dimer **3b** as a white crystalline powder (30.5 mg, 0.022 mmol, 54%). The sample of **3b** thus obtained was spectroscopically pure, although elemental analysis could not be performed because of its high sensitivity toward oxygen and moisture. ^1H NMR (r.t., toluene- d_8): δ 7.41 (d, $^3J = 6.5$ Hz, 16H, Si–Ph(*o*)), 7.17–7.12 (m, 12H, Si–Ph(*p*) + C(3)–H), 7.10–7.03 (m, 20H, Si–Ph(*m*) + C(5)–H), 4.94 (brs, 2H, CH_2), 3.28 (brs, 2H, CH_2), 2.03 (s, 12H, ArMe), 0.72 (s, 12H, SiMe); ^1H NMR (–60 °C, toluene- d_8): δ 7.53 (d, $^3J = 6.6$ Hz, 8H, Si–Ph(*o*)), 7.44 (d, $^3J = 7.0$ Hz, 4H, Si–Ph(*o*)), 7.31 (s, 2H, C(3)–H), 7.26–7.06 (m, 30H, Si–Ph + C(3)–H + C(5)–H), 6.89 (t, $^3J = 7.2$ Hz, 4H, Si–Ph(*m*)), 6.36 (brd, $^3J = 12$ Hz, 2H, CH_2), 3.34 (brd, $^3J = 12$ Hz, 2H, CH_2), 2.07 (s, 6H, ArMe), 1.89 (s, 6H, ArMe), 0.80 (s, 6H, SiMe), 0.46 (s, 6H, SiMe); $^{13}\text{C}\{^1\text{H}\}$ NMR (r.t., toluene- d_8): δ 157.6 (s, 4°, C(1)–OH), 138.0 (brs, 4°, C(*ipso*) of SiPh), 136.4 (s, 3°, C(5)), 135.5 (s, 3°, C(*o*) of SiPh), 133.9 (s, 3°, C(3)), 133.2 (brs, 4°, C(2)), 131.2 (brs, 4°, C(4)), 129.4 (s, 3°, C(*p*) of SiPh), 128.4 (s, 3°, C(*m*) of SiPh), 126.3 (brs, 4°, C(6)), 35.0 (s, 2°, CH_2), 20.7 (s, 1°, ArMe), –1.2 (s, 1°, SiMe); ^{29}Si NMR (toluene- d_8): δ –5.5 (s).

2.8. Single-Crystal XRD Analysis

Diffraction data for **3a–b** were collected on a VariMax Saturn CCD diffractometer with graphite-monochromated Mo $K\alpha$ radiation ($\lambda = 0.71075$ Å) at –180 °C. Intensity data were corrected for Lorentz-polarization effects and for empirical absorption (REQAB) [39]. Calculations were performed using the CrystalStructure [40] and OLEX2 crystallographic [41,42] software packages except for refinements, which were performed using SHELXL-2018/3 [43]. All non-hydrogen atoms were refined on F_o^2 anisotropically using full-matrix least-square techniques. All hydrogen atoms were placed at the calculated positions with fixed isotropic parameters.

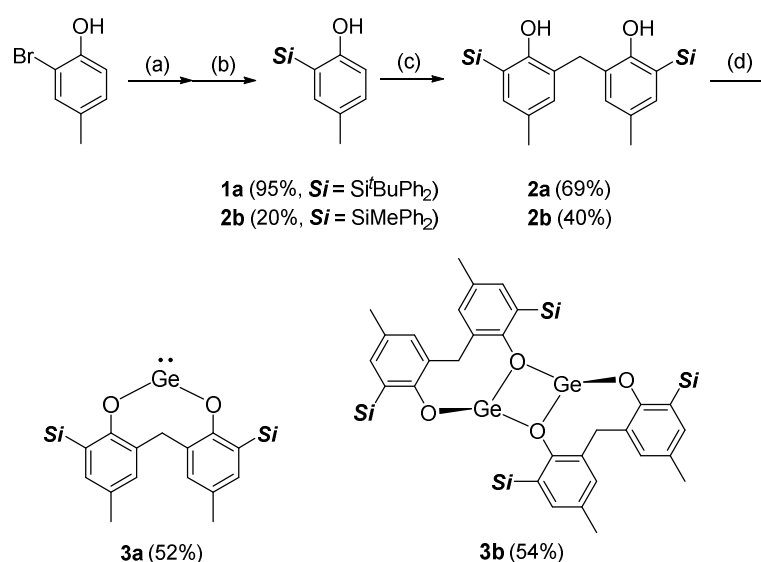
Crystal Data for $\text{C}_{47}\text{H}_{50}\text{GeO}_2\text{Si}_2$ (**3a**) (M = 775.703 g/mol): triclinic, space group *P*-1 (no. 2), $a = 10.745(2)$ Å, $b = 13.378(3)$ Å, $c = 14.756(3)$ Å, $\alpha = 79.564(11)^\circ$, $\beta = 76.944(10)^\circ$, $\gamma = 78.66(1)^\circ$, $V = 2005.0(7)$ Å³, $Z = 2$, $T = 93(2)$ K, $\mu(\text{MoK}\alpha) = 0.71075$ mm^{–1}, $D_{\text{calc}} = 1.285$ g/cm³, 16,588 reflections measured ($7.1^\circ \leq 2\theta \leq 54.9^\circ$), 8827 unique ($R_{\text{int}} = 0.046$) which were used in all calculations. The final R_1 was 0.0657 ($I > 2\sigma(I)$) and wR_2 was 0.1691 (all data).

Crystal Data for $C_{82}H_{76}Ge_2O_4Si_4$ (**3b**) ($M = 1383.01$ g/mol): orthorhombic, space group $Pca2_1$ (no. 29), $a = 27.190(6)$ Å, $b = 10.177(2)$ Å, $c = 25.324(6)$ Å, $V = 7008(3)$ Å³, $Z = 4$, $T = 93(2)$ K, $\mu(\text{MoK}\alpha) = 0.71075$ mm⁻¹, $D_{\text{calc}} = 1.311$ g/cm³, 54,569 reflections measured ($6.0^\circ \leq 2\Theta \leq 55.0^\circ$), 15,982 unique ($R_{\text{int}} = 0.1268$) which were used in all calculations. The final R_1 was 0.1074 ($I > 2\sigma(I)$) and wR_2 was 0.2835 (all data).

3. Results and Discussion

3.1. Synthesis

Scheme 1 illustrates the synthetic route to novel diaryloxygermylenes from commercially available 2-bromo-4-methylphenol. The *O*-silylation of the cresol followed by retro-Brook rearrangement provided 2-silyl-4-methylphenols **1a–b** [44,45], which are transformed into the corresponding 2,2'-methylene-diphenols **2a–b** in moderate yields [33,46]. Treatment of $Ge[N(\text{SiMe}_3)_2]_2$ and **2a–b** in hexane at 50 °C resulted in the formation of diaryloxygermylene **3a** and dimer **3b**, respectively, as a white powder. Although the isolated yields of **3a** and **3b** are not high, nearly quantitative formation of these products has been confirmed by the ¹H NMR spectra of the crude products.



Scheme 1. Synthetic route to diaryloxygermylenes **3a–b** from 2-bromo-4-methylphenol. (a) imidazole (4 equiv), ^tBuPh₂SiCl or MePh₂SiCl (1.1 equiv), CH₂Cl₂, r.t. or 40 °C, 24 h. (b) ⁿBuLi (1.1 equiv), THF, –78 °C, 30 min., then r.t. for 24 h. (c) MeMgBr (1 equiv), Et₂O, 0 °C to r.t., 30 min., then (CH₂O)_n (0.5 equiv), toluene, 80 °C, 24 h. (d) $Ge[N(\text{SiMe}_3)_2]_2$, hexane, 50 °C.

3.2. Solid-State Structures

Slow cooling of hot hexane solution of **3a** provided colorless single-crystals, whereas slow diffusion of pentane into a toluene solution of **3b** deposited colorless crystals. X-ray diffraction analysis of these crystals revealed their solid-state structures as shown in Figures 1 and 2, although the data of **3b** should be regarded as preliminary results because of the high wR_2 value.

In **3a**, the Ge–O1/2 bond lengths are nearly identical (1.820(3)/1.829(3) Å), and the O1–Ge–O2 angle is 99.89(11)°. This angle is larger than the O–Ge–O angles found in monomeric $Ge^{II}(\text{OR})_2$ type germylenes (85–92°) [13,23,24,47,48], although smaller than the angle in a related compound with a Ge(IV) center (107.5°) [49]. Notably, the closest Ge...O2 distance in the packing structure is 3.0292(3) Å, significantly longer than those in well-known dimers of dioxygermylenes (ca. 1.98 Å) [13,48]. However, considering that the sum of the van der Waals radii of Ge and O atoms is 3.63 Å [50], the solid-state structure of **3a** can be best described as a weakly bound dimer. To the best of our knowledge, such dimeric structure with relatively large Ge...O separation, yet within the sum of the van der

Waals radii, is unprecedented in the family of dioxytetrylenes reported so far. In fact, most dioxytetrylenes exist as monomers or tightly bound dimers in the crystalline state, and weakly bound dimeric structures of dioxytetrylenes have never been reported. It should also be mentioned that the weakly bound dimer possesses a crystallographic center of symmetry, and therefore two 2,2'-methylenebisphenol moieties are located mutually trans with respect to the Ge_2O_2 tetragon.

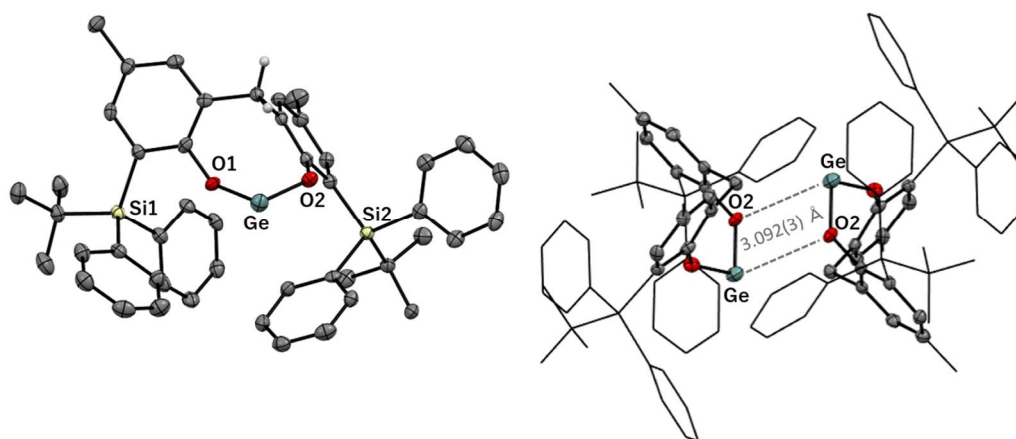


Figure 1. Solid-state structures of **3a** with thermal ellipsoid plots at 50% probability. All hydrogen atoms except for those of the methylene in the left figure are omitted for clarity. **Left:** monomeric structure. **Right:** two closest germylene units in the packing structure. The Si^tBuPh_2 and Me groups are shown in wireframe.

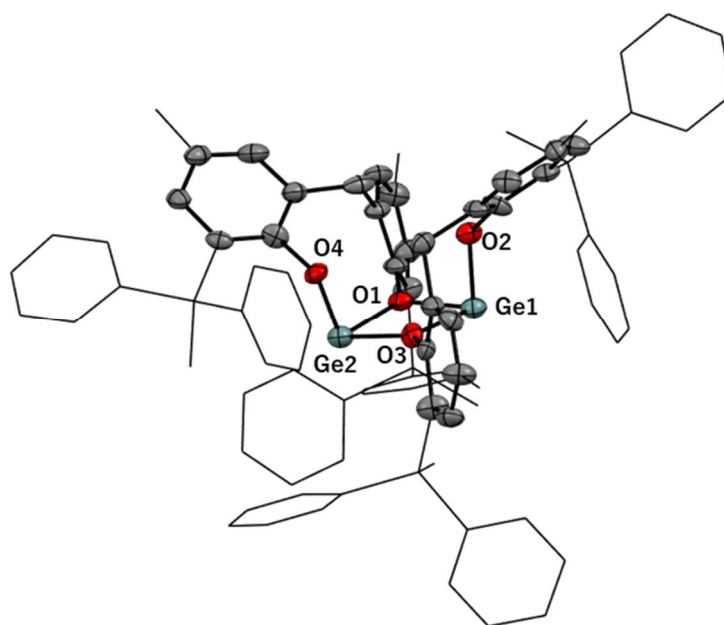


Figure 2. Solid-state structure of **3b** with thermal ellipsoid plots at 50% probability. All hydrogen atoms are omitted for clarity. The SiMePh_2 and Me groups are shown in wireframe.

In contrast to the loosely bound dimer in **3a**, compound **3b** forms a tightly bound dimer as illustrated in Figure 2. The average $\text{Ge}-\text{O}_{\text{terminal}}$ bond length ($\text{Ge1}-\text{O2}$ and $\text{Ge2}-\text{O4}$; 1.814(6) Å) is shorter than the average $\text{Ge}-\text{O}_{\text{bridging}}$ bond ($\text{Ge1}-\text{O1}$, $\text{Ge1}-\text{O3}$, $\text{Ge2}-\text{O1}$, and $\text{Ge2}-\text{O3}$; 2.010(6) Å) as was found in the related diaryloxygermylene dimers [13,48]. The $\text{O2}-\text{Ge1}-\text{O3}$ and $\text{O1}-\text{Ge2}-\text{O4}$ angles are 95.6(3) and 97.6(3)°, slightly smaller than that of **3a** (99.89(11)°). The terminal aryloxy groups are arranged in a cis fashion, which is also an uncommon feature in the family of dioxytetrylenes; most dimers of dioxytetrylenes

have trans-orientated terminal O-substituents, and only a few examples have been reported to possess crystal structure of cis-oriented dioxytetrylene dimers [48,51,52]. Because of the cis-orientation, one of the methylene protons in a dioxygermylene unit is spatially close to the oxygen atom of the other, which enables CH...O hydrogen bonding. Indeed, the distances between the methylene CH...O_{terminal} are 2.25(1) and 2.46(1) Å, and the C–H–O angles are 142(1) and 151.8(9)° (Supplementary Materials Figure S1), within the normal range for CH...O hydrogen bonding [53–55].

3.3. NMR Studies

To investigate the solution behavior of **3a** and **3b**, VT-¹H NMR spectra were recorded in toluene-*d*₈ (Figures S2–S4). In the ¹H NMR spectra of **3a** at 20 °C, only one broad methylene signal with a half width of ca. 50 Hz is observed at δ 3.36, indicating that the inversion of the central eight-membered C₅O₂Ge ring occurs slowly at this temperature (Figure S5). Upon cooling to 0 °C, the methylene signal splits into two broad signals (δ 3.46, 3.20), which are observed as two sharp doublets (δ 3.46, 3.21) with a coupling constant of ca. 14 Hz below –40 °C (Figure S2). Thus, the ring inversion is frozen at lower temperatures. Accordingly, two sets of SiPh signals were observed below –40 °C because of their diastereotopic nature. It should be noted that only one set of ¹H NMR signals originating from the two aryloxy groups is observed over the temperature range –80 to 20 °C, which is not the case for **3b** as mentioned below. These observations clearly indicate that **3a** exists substantially as a monomeric germylene in the solution state.

The ¹H NMR spectrum of **3b** at 20 °C exhibits one set of aryloxy signals, e.g., δ 0.72 (SiMe) and 2.03 (ArMe), indicating a fluxional nature of the dimer structure (Figure S5), and two broadened methylene signals (δ 4.94 and 3.28) as shown in Figures S3 and S4. The latter methylene signals coalesce at 40 °C and change to a broad singlet at δ 3.65 at 60 °C, revealing that the ring inversion in **3b** requires higher energy than that in **3a**. This difference implies that the solution behavior of **3a** and **3b** is different; it is highly likely that dimeric structure of **3b** is maintained in solution, while it undergoes partial dissociation and ring inversion at or above r.t., which explains the fluxionality. In fact, in the ¹H NMR spectrum of **3b** at –80 °C, two sets of aryloxy signals are observed, for instance, δ 0.84 and 0.41 for the SiMe groups, with an integration ratio of 1:1. This nonequivalence of the two aryloxy groups can be reasonably explained by assuming that the Ge₂O₂ dimeric core is rigid and no exchange takes place between the terminal and bridging aryloxy groups at –80 °C. To our surprise, one of the methylene signals exhibits a significant downfield shift upon cooling (δ 4.94 (20 °C), 5.47 (0 °C), 5.95 (–20 °C), 6.30 (–40 °C), 6.36 (–60 °C), 6.43 (–80 °C)), which is in contrast to the normal chemical shifts for the methylene in **3a** (δ 3.46, 3.20 at –60 °C). We infer that the origin of the downfield shifts is the CH...O hydrogen bonding in the cis-oriented dimeric structure [56–58].

4. Conclusions

Novel two aryloxygermylenes **3a–b** derived from 2,2'-methylenediphenols have been synthesized and structurally characterized. Compound **3a** crystalizes as a weakly bound dimer that is unprecedented in the structures of dioxytetrylenes reported so far, whereas **3b** has a tightly bound rhombic Ge₂O₂ ring with cis-oriented terminal aryloxy groups. The VT-NMR studies unveiled that **3a** and **3b** exist as a monomer and a dimer, respectively, in solution. These structural differences stem from the different bulkiness between Si^{*i*}BuPh₂ and SiMePh₂ at the 6 and 6'-positions of the 2,2'-methylenediphenoxide ligand.

Supplementary Materials: The following supporting information can be downloaded at: <https://www.mdpi.com/article/10.3390/cryst12050605/s1>, Figure S1: Hydrogen bonds in **3b**; Figures S2–S4: VT-NMR spectra; Figure S5: dynamic behaviors of **3a,b**; Table S1: Crystal data for **3a,b**; Figures S6–S20: NMR spectra of new compounds.

Author Contributions: Conceptualization, T.K.; investigation, R.Y., R.K. and A.S.; validation, T.K. and Y.I.; writing—original draft preparation, T.K.; writing—review and editing, Y.I.; project administration, T.K. and Y.I.; funding acquisition, T.K. and Y.I. All authors have read and agreed to the published version of the manuscript.

Funding: This research was funded by JSPS KAKENHI, grant number 20K15265.

Institutional Review Board Statement: Not applicable.

Data Availability Statement: CCDC 2159874 (3a), 2159875 (3b) contain the supplementary crystallographic data for this paper. These data can be obtained free of charge via www.ccdc.cam.ac.uk/data_request/cif (accessed on 24 April 2022), or by emailing data_request@ccdc.cam.ac.uk, or by contacting The Cambridge Crystallographic Data Centre, 12 Union Road, Cambridge CB2 1EZ, U.K.; Fax: +44 1223 336033.

Conflicts of Interest: The authors declare no conflict of interest.

References and Note

1. Mizuhata, Y.; Sasamori, T.; Tokitoh, N. Stable Heavier Carbene Analogues. *Chem. Rev.* **2009**, *109*, 3479–3511. [[CrossRef](#)]
2. Power, P.P. Main-group elements as transition metals. *Nature* **2010**, *463*, 171–177. [[CrossRef](#)]
3. Hadlington, T.J.; Driess, M.; Jones, C. Low-valent group 14 element hydride chemistry: Towards catalysis. *Chem. Soc. Rev.* **2018**, *47*, 4176–4197. [[CrossRef](#)]
4. Shan, C.; Yao, S.; Driess, M. Where silylene–silicon centres matter in the activation of small molecules. *Chem. Soc. Rev.* **2020**, *49*, 6733–6754. [[CrossRef](#)]
5. Davidson, P.J.; Lappert, M.F. Stabilisation of metals in a low co-ordinative environment using the bis(trimethylsilyl)methyl ligand; coloured Sn and Pb alkyls, $M[CH(SiMe_3)_2]_2$. *J. Chem. Soc. Chem. Commun.* **1973**, 317a. [[CrossRef](#)]
6. Harris, D.H.; Lappert, M.F. Monomeric, volatile bivalent amides of group IV elements, $M(NR^{12})_2$ and $M(NR^1R^2)_2$ ($M = Ge, Sn, or Pb$; $R^1 = Me_3Si, R^2 = Me_3C$). *J. Chem. Soc. Chem. Commun.* **1974**, 895–896. [[CrossRef](#)]
7. McCrea-Hendrick, M.L.; Bursch, M.; Gullett, K.L.; Maurer, L.R.; Fettingner, J.C.; Grimme, S.; Power, P.P. Counterintuitive Interligand Angles in the Diaryls $E[C_6H_3-2,6-(C_6H_2-2,4,6-^iPr_3)_2]_2$ ($E = Ge, Sn, or Pb$) and Related Species: The Role of London Dispersion Forces. *Organometallics* **2018**, *37*, 2075–2085. [[CrossRef](#)]
8. Perla, L.G.; Kulenkampff, J.M.; Fettingner, J.C.; Power, P.P. Steric and Electronic Properties of the Bulky Terphenyl Ligand ArtBu6 ($Ar^{tBu6} = C_6H_3-2,6-(C_6H_2-2,4,6-^iBu_3)_2$) and Synthesis of Its Tin Derivatives $Ar^{tBu6}SnCl$, $Ar^{tBu6}SnSn(H)_2Ar^{tBu6}$, and $Ar^{tBu6}SnSnAr^{tBu6}$: A New Route to a Distannyne via Thermolysis of the Asymmetric Hydride $Ar^{tBu6}SnSn(H)_2Ar^{tBu6}$. *Organometallics* **2018**, *37*, 4048–4054.
9. Matsuo, T.; Tamao, K. Fused-Ring Bulky “Rind” Groups Producing New Possibilities in Elemento-Organic Chemistry. *Bull. Chem. Soc. Jpn.* **2015**, *88*, 1201–1220. [[CrossRef](#)]
10. Suzuki, F.; Nishino, R.; Yukimoto, M.; Sugamata, K.; Minoura, M. Synthesis, Structure, and Reactivity of a Thermally Stable Dialkylgermylene. *Bull. Chem. Soc. Jpn.* **2020**, *93*, 249–251. [[CrossRef](#)]
11. Protchenko, A.V.; Birjkumar, K.H.; Dange, D.; Schwarz, A.D.; Vidovic, D.; Jones, C.; Kaltsoyannis, N.; Mountford, P.; Aldridge, S. A Stable Two-Coordinate Acyclic Silylene. *J. Am. Chem. Soc.* **2012**, *134*, 6500–6503. [[CrossRef](#)]
12. Protchenko, A.V.; Dange, D.; Schwarz, A.D.; Tang, C.Y.; Phillips, N.; Mountford, P.; Jones, C.; Aldridge, S. Heavy metal boryl chemistry: Complexes of cadmium, mercury and lead. *Chem. Commun.* **2014**, *50*, 3841–3844. [[CrossRef](#)]
13. Weinert, C.S.; Fenwick, A.E.; Fanwick, P.E.; Rothwell, I.P. Synthesis, structures and reactivity of novel germanium(ii) aryloxide and arylsulfide complexes. *Dalton Trans.* **2003**, 532–539. [[CrossRef](#)]
14. Goel, S.C.; Chiang, M.Y.; Buhro, W.E. Preparation of six lead(II) dialkoxides, X-ray crystal structures of $[Pb(\mu, \eta^1-OCH_2CH_2OMe)_2]_\infty$ and $[Pb_3(\mu-O-tert-Bu)_6]$, and hydrolysis studies. *Inorg. Chem.* **1990**, *29*, 4640–4646. [[CrossRef](#)]
15. Kitschke, P.; Ruffer, T.; Korb, M.; Lang, H.; Schneider, W.B.; Auer, A.A.; Mehring, M. Intramolecular C–O Insertion of a Germanium(II) Salicyl Alcoholate: A Combined Experimental and Theoretical Study. *Eur. J. Inorg. Chem.* **2015**, *2015*, 5467–5479. [[CrossRef](#)]
16. Kitschke, P.; Walter, M.; Ruffer, T.; Seifert, A.; Speck, F.; Seyller, T.; Spange, S.; Lang, H.; Auer, A.A.; Kovalenko, M.V.; et al. Porous Ge@C materials via twin polymerization of germanium(ii) salicyl alcoholates for Li-ion batteries. *J. Mater. Chem. A* **2016**, *4*, 2705–2719. [[CrossRef](#)]
17. Boyle, T.J.; Doan, T.Q.; Steele, L.A.M.; Apblett, C.; Hoppe, S.M.; Hawthorne, K.; Kalinich, R.M.; Sigmund, W.M. Tin(ii) amide/alkoxide coordination compounds for production of Sn-based nanowires for lithium ion battery anode materials. *Dalton Trans.* **2012**, *41*, 9349–9364. [[CrossRef](#)]
18. Stanciu, C.; Richards, A.F.; Stender, M.; Olmstead, M.M.; Power, P.P. New terphenylphenoxides of group 13 and 14 elements. *Polyhedron* **2006**, *25*, 477–483. [[CrossRef](#)]
19. Dickie, D.A.; MacIntosh, I.S.; Ino, D.D.; He, Q.; Labeodan, O.A.; Jennings, M.C.; Schatte, G.; Walsby, C.J.; Clyburne, J.A.C. Synthesis of the bulky *m*-terphenyl phenol Ar^*OH ($Ar^* = C_6H_3-2,6-Mes_2$, $Mes = 2,4,6$ -trimethylphenyl) and the preparation and structural characterization of several of its metal complexes. *Can. J. Chem.* **2008**, *86*, 20–31. [[CrossRef](#)]

20. Rekken, B.D.; Brown, T.M.; Olmstead, M.M.; Fettinger, J.C.; Power, P.P. Stable Plumbylene Dichalcogenolate Monomers with Large Differences in Their Interligand Angles and the Synthesis and Characterization of a Monothiolato Pb(II) Bromide and Lithium Trithiolato Plumbate. *Inorg. Chem.* **2013**, *52*, 3054–3062. [[CrossRef](#)]
21. Rekken, B.D.; Brown, T.M.; Fettinger, J.C.; Lips, F.; Tuononen, H.M.; Herber, R.H.; Power, P.P. Dispersion Forces and Counterintuitive Steric Effects in Main Group Molecules: Heavier Group 14 (Si–Pb) Dichalcogenolate Carbene Analogues with Sub-90° Interligand Bond Angles. *J. Am. Chem. Soc.* **2013**, *135*, 10134–10148. [[CrossRef](#)]
22. Cetinkaya, B.; Gumrukcu, I.; Lappert, M.F.; Atwood, J.L.; Rogers, R.D.; Zaworotko, M.J. Bivalent germanium, tin, and lead 2,6-di-*tert*-butylphenoxides and the crystal and molecular structures of $M(\text{OC}_6\text{H}_2\text{Me-4-Bu}^t\text{-2,6})_2$ ($M = \text{Ge}$ or Sn). *J. Am. Chem. Soc.* **1980**, *102*, 2088–2089. [[CrossRef](#)]
23. Gerung, H.; Boyle, T.J.; Tribby, L.J.; Bunge, S.D.; Brinker, C.J.; Han, S.M. Solution Synthesis of Germanium Nanowires Using a Ge^{2+} Alkoxide Precursor. *J. Am. Chem. Soc.* **2006**, *128*, 5244–5250. [[CrossRef](#)]
24. Weinert, C.S.; Fanwick, P.E.; Rothwell, I.P. Novel germanium(ii) binaphthoxide complexes: Synthesis and crystal structure of (*R,R*)-[Ge(OC₂₀H₁₀(OSiMe₃)-2'-3,3')₂] and (*R*)-[Ge(O₂C₂₀H₁₀(SiMe₂Ph)₂-3,3')₂]{NH₃}; catalytic function of Ge[N(SiMe₃)₂]₂ for the mono-silylation of 3,3'-disubstituted-1,1'-bi-2,2'-naphthols. *J. Chem. Soc. Dalton Trans.* **2002**, 2948–2950. [[CrossRef](#)]
25. Someşan, A.-A.; Le Coz, E.; Roisnel, T.; Silvestru, C.; Sarazin, Y. Stable lead(ii) boroxides. *Chem. Commun.* **2018**, *54*, 5299–5302. [[CrossRef](#)]
26. Loh, Y.K.; Ying, L.; Fuentes, M.Á.; Do, D.C.H.; Aldridge, S. An N-Heterocyclic Boryloxy Ligand Isoelectronic with N-Heterocyclic Imines: Access to an Acyclic Dioxysilylene and its Heavier Congeners. *Angew. Chem., Int. Ed.* **2019**, *58*, 4847–4851. [[CrossRef](#)] [[PubMed](#)]
27. Kuriki, R.; Kuwabara, T.; Ishii, Y. Synthesis and structures of diaryloxystannylenes and -plumbylenes embedded in 1,3-diethers of thiocalix [4]arene. *Dalton Trans.* **2020**, *49*, 12234–12241. [[CrossRef](#)] [[PubMed](#)]
28. Hascall, T.; Parkin, G.; Hascall, T.; Rheingold, A.L.; Guzei, I. Subvalent germanium and tin complexes supported by a dianionic calixarene ligand: Structural characterization of *exo* and *endo* isomers of [Bu^tcalix^(TMS)]₂Ge. *Chem. Commun.* **1998**, 101–102. [[CrossRef](#)]
29. Hascall, T.; Pang, K.; Parkin, G. *exo* and *endo* Isomerism of subvalent tin and germanium complexes derived from 1,3-diethers of *p-tert*-butylcalix [4]arene. *Tetrahedron* **2007**, *63*, 10826–10833. [[CrossRef](#)]
30. McBurnett, B.G.; Cowley, A.H. Binuclear tin and germanium calix [4]arenes. *Chem. Commun.* **1999**, 17–18. [[CrossRef](#)]
31. Wetherby, A.E.; Goeller, L.R.; DiPasquale, A.G.; Rheingold, A.L.; Weinert, C.S. Synthesis and Structures of an Unusual Germanium(II) Calix [4]arene Complex and the First Germanium(II) Calix [8]arene Complex and Their Reactivity with Diiron Nonacarbonyl. *Inorg. Chem.* **2007**, *46*, 7579–7586. [[CrossRef](#)] [[PubMed](#)]
32. Schrick, A.C.; Rheingold, A.L.; Weinert, C.S. A divalent germanium complex of calix [5]arene. *Dalton Trans.* **2011**, *40*, 6629–6631. [[CrossRef](#)] [[PubMed](#)]
33. Davis, T.J.; Balsells, J.; Carroll, P.J.; Walsh, P.J. Optimization of Asymmetric Catalysts Using Achiral Ligands: Metal Geometry-Induced Ligand Asymmetry. *Org. Lett.* **2001**, *3*, 2161–2164. [[CrossRef](#)] [[PubMed](#)]
34. Kawaguchi, H.; Matsuo, T. Aryloxy-based multidentate ligands for early transition metals and f-element metals. *J. Organomet. Chem.* **2004**, *689*, 4228–4243. [[CrossRef](#)]
35. Watanabe, T.; Ishida, Y.; Matsuo, T.; Kawaguchi, H. Reductive Coupling of Six Carbon Monoxides by a Ditantalum Hydride Complex. *J. Am. Chem. Soc.* **2009**, *131*, 3474–3475. [[CrossRef](#)]
36. Buccella, D.; Tanski, J.M.; Parkin, G. Factors Influencing Coordination versus Oxidative Addition of C–H Bonds to Molybdenum and Tungsten: Structural and Spectroscopic Evidence That the Calixarene Framework Promotes C–H Bond Activation. *Organometallics* **2007**, *26*, 3275–3278. [[CrossRef](#)]
37. Ishida, Y.; Kawaguchi, H. Methylene-Linked Anilide–Bis(aryloxy) Ligands: Lithium, Sodium, Potassium, Chromium(III), and Vanadium(III) Ligation. *Inorg. Chem.* **2014**, *53*, 6775–6787. [[CrossRef](#)]
38. Kuwabara, T.; Toriumi, T.; Suzuki, M.; Ishii, Y. Selective Double CH Activation at a Methylene Carbon in Methylene-diphenol Derivatives to Generate Carbene-Bridged Dinuclear Iridium Complexes. *Organometallics* **2020**, *39*, 4500–4509. [[CrossRef](#)]
39. Jacobson, R.A. *Private Communication to Rigaku Corp.*; Rigaku Corp.: Tokyo, Japan, 1998.
40. *Crystal Structure 4.0: Single Crystal Structure Analysis Package*; Rigaku Corp.: Tokyo, Japan, 2000–2010.
41. Dolomanov, O.V.; Bourhis, L.J.; Gildea, R.J.; Howard, J.A.K.; Puschmann, H. OLEX2: A complete structure solution, refinement and analysis program. *J. Appl. Cryst.* **2009**, *42*, 339–341. [[CrossRef](#)]
42. Bourhis, L.J.; Dolomanov, O.V.; Gildea, R.J.; Howard, J.A.K.; Puschmann, H. The anatomy of a comprehensive constrained, restrained refinement program for the modern computing environment-Olex2 dissected. *Acta Crystallogr. Sec. A* **2015**, *71*, 59–75. [[CrossRef](#)]
43. Sheldrick, G. Crystal structure refinement with SHELXL. *Acta Crystallogr. Sec. C* **2015**, *71*, 3–8. [[CrossRef](#)] [[PubMed](#)]
44. Simchen, G.; Pfletschinger, J. Anionic O → C Rearrangements in Trialkylsiloxy-benzenes and Trialkylsiloxy-pyridines. *Angew. Chem. Int. Ed. Engl.* **1976**, *15*, 428–429. [[CrossRef](#)]
45. Ikawa, T.; Nishiyama, T.; Nosaki, T.; Takagi, A.; Akai, S. A Domino Process for Benzyne Preparation: Dual Activation of *o*-(Trimethylsilyl)phenols by Nonfluorobutanesulfonyl Fluoride. *Org. Lett.* **2011**, *13*, 1730–1733. [[CrossRef](#)]
46. Casiraghi, G.; Casnati, G.; Cornia, M.; Pochini, A.; Puglia, G.; Sartori, G.; Ungaro, R. Selective reactions using metal phenoxides. Part 1. Reactions with formaldehyde. *J. Chem. Soc. Perkin Trans. 1* **1978**, 318–321. [[CrossRef](#)]

47. Fjeldberg, T.; Hitchcock, P.B.; Lappert, M.F.; Smith, S.J.; Thorne, A.J. Chemistry of bulky alkoxides of bivalent germanium and tin; structures of gaseous $[\text{Sn}(\text{O}^t\text{Bu})_2]_2$ and crystalline $\text{Ge}(\text{OC}^t\text{Bu})_2$. *J. Chem. Soc. Chem. Commun.* **1985**, 939–941. [[CrossRef](#)]
48. Boyle, T.J.; Tribby, L.J.; Ottley, L.A.M.; Han, S.M. Synthesis and Characterization of Germanium Coordination Compounds for Production of Germanium Nanomaterials. *Eur. J. Inorg. Chem.* **2009**, 2009, 5550–5560. [[CrossRef](#)]
49. Khoury, N.; Pastor, S.D.; Rahni, D.; Richardson, C.F.; Syed, N.A.; Shum, S.P.; Chandrasekaran, A. The Conformation of Sterically Congested Eight-membered Rings Containing Germanium: First X-ray Crystallographic Characterization of the Boat Conformation. *Phosphorus Sulfur Silicon Relat. Elem.* **2004**, 179, 483–497. [[CrossRef](#)]
50. Mantina, M.; Chamberlin, A.C.; Valero, R.; Cramer, C.J.; Truhlar, D.G. Consistent van der Waals Radii for the Whole Main Group. *J. Phys. Chem. A* **2009**, 113, 5806–5812. [[CrossRef](#)]
51. Veith, M.; Belot, C.; Huch, V.; Zimmer, M. Influence of the Solvent on the Formation of New Tin(II) Methoxides Containing Thienyl Substituents: Crystal Structure and NMR Investigations. *Z. Anorg. Allg. Chem.* **2009**, 635, 942–948. [[CrossRef](#)]
52. Hill, M.S.; Johnson, A.L.; Lowe, J.P.; Molloy, K.C.; Parish, J.D.; Wildsmith, T.; Kingsley, A.L. Aerosol-assisted CVD of SnO from stannous alkoxide precursors. *Dalton Trans.* **2016**, 45, 18252–18258. [[CrossRef](#)]
53. Desiraju, G.R. The C–H \cdots O hydrogen bond in crystals: What is it? *Acc. Chem. Res.* **1991**, 24, 290–296. [[CrossRef](#)]
54. Steiner, T. Unrolling the hydrogen bond properties of C–H \cdots O interactions. *Chem. Commun.* **1997**, 727–734. [[CrossRef](#)]
55. Steiner, T. C–H \cdots O hydrogen bonding in crystals. *Crystallogr. Rev.* **2003**, 9, 177–228. [[CrossRef](#)]
56. Ash, E.L.; Sudmeier, J.L.; Day, R.M.; Vincent, M.; Torchilin, E.V.; Haddad, K.C.; Bradshaw, E.M.; Sanford, D.G.; Bachovchin, W.W. Unusual ^1H NMR chemical shifts support (His) $\text{C}^{\epsilon 1}\text{--H}\cdots\text{O}=\text{C}$ H-bond: Proposal for reaction-driven ring flip mechanism in serine protease catalysis. *Proc. Natl. Acad. Sci. USA* **2000**, 97, 10371–10376. [[CrossRef](#)]
57. Vibhute, A.M.; Deva Priyakumar, U.; Ravi, A.; Sureshan, K.M. Model molecules to classify CH \cdots O hydrogen-bonds. *Chem. Commun.* **2018**, 54, 4629–4632. [[CrossRef](#)]
58. Since such downfield shifts have also been observed for a related tin compound having Si^iPr_3 substituents instead of SiMePh_2 and Si^tBuPh_2 , we exclude the possibility that the downfield shifts are caused by ring currents of the Ph rings.